Appl Biol Chem (2017) 60(6):637–645
DOI 10.1007/s13765-017-0321-9

Online ISSN 2468-0842
Print ISSN 2468-0834

ARTICLE

Development of a colorimetric nucleic acid-based lateral flow assay with non-biotinylated capture DNA

Atefeh Javani[1] · Fatemeh Javadi-Zarnaghi[1] · Mohammad Javad Rasaee[2]

Received: 14 July 2017 / Accepted: 19 September 2017 / Published online: 30 September 2017

Abstract In recent years, many nucleic acid-based lateral flow assays (NALFAs) have been developed for rapid and simple detection of various analytes including DNA sequences. In a NALFA, target molecules are applied within a small volume of a rehydrating buffer. The analyte flows laterally to reach the capture molecules at where it forms a colorimetric signal. Usually, in NALFAs, capture molecules are modified for maximized adsorption on the surface. In most cases, the modification is a biotin. The biotinylated capture DNA is held at capture line by interaction with streptavidin. However, there is a demand on methods that permit utilizing unmodified capture molecules and allow a cost-effective development process. Here, we report on a biotin- and streptavidin-free model NALFA. We also present a systematic investigation on the effect of various rehydrating buffers' composition and concentration. In addition, the impacts of a protein blocker, detergents and chaotropic and kosmotropic agents on the intensity of the signal over background were analyzed. It has been demonstrated that simultaneous presence of sodium dodecyl sulfate and bovine serum albumin doubles the intensity of visible bands in the presented unmodified NALFA. Finally, this paper presents an optimized cost-effective model system that can be adapted for hybridization-based NALFAs.

✉ Fatemeh Javadi-Zarnaghi
fa.javadi@sci.ui.ac.ir

[1] Department of Biology, Faculty of Sciences, University of Isfahan, Isfahan, Iran

[2] Department of Medical Biotechnology, Faculty of Medical Sciences, Tarbiat Modares University, Tehran, Iran

Keywords Biotin–streptavidin · Lateral flow assays · Nucleic acid · Protein-free nucleic acid-based lateral flow assay · Rehydrating buffer

Introduction

Rapid and simple, one-step assays that support application at points of care (POC) have got more attentions in recent years [1–3]. These tests do not require high-tech instrumentation and are easy to be applied by non-specialized people. A major class of POC tests are lateral flow assays (LFA) [1]. Home pregnancy test devices that analyze presence of β-hCG in human urine are well-known examples of LFA. However, LFAs are not limited in respect of their target molecules. LFAs detect a wide range of targets including health biomarkers [4], pathogens [5] and toxins [6].

LFAs consist of four different membranes which are embedded laterally. The four membranes are sample pad, conjugate release pad, nitrocellulose membrane and wicking pad. Biological liquids such as blood [2], plasma [7], serum [8], urine [9], saliva [3] or extracts from agricultural products [10], drinking water [11], milk and fruit juice [12] are common samples that are applied onto the sample pad. Conjugate release pad provides a membrane for settlement of color-inducing substances. Gold nanoparticles are one of the major color-inducing substances in LFAs and are conjugated with the detector macromolecule. The detector macromolecule is either an antibody or oligonucleotide. Upon applying sample, the capillary forces transfer the sample liquid to the wicking pad via conjugate release pad and nitrocellulose membrane. Lateral migration of the sample liquid to the nitrocellulose membrane brings the gold nanoparticle detector conjugates, named "conjugates"

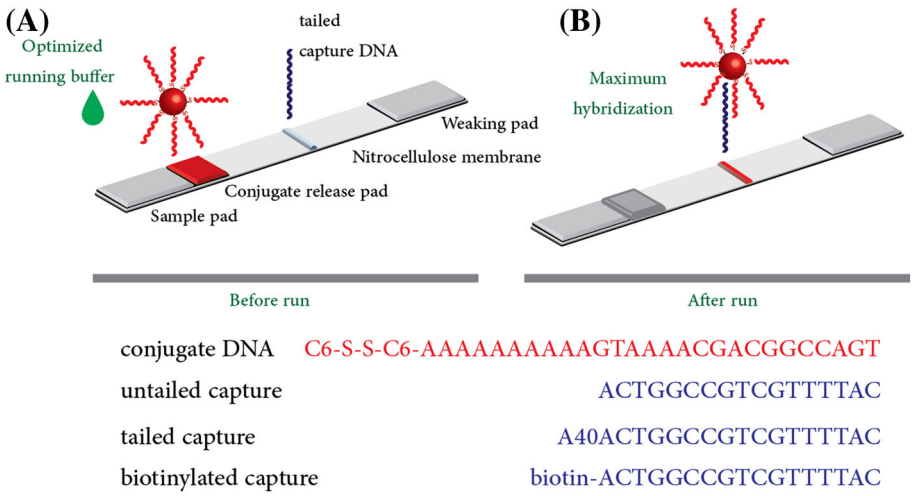

Fig. 1 General scheme. General schematic view of the model NALFA that is presented in this study prior and after applying the rehydrating buffer. DNA sequences of this study are marked below the scheme. The biotinylated capture DNA is used as a control

from here, in vicinity of "capture molecules" at the control and test lines. Capture molecules are immobilized species on nitrocellulose membrane and are designed to couple to conjugates upon presence of the target in direct assays [13]. The conjugates pass the capture molecules at test line, in competitive assays [14].

The capture molecules at the control lines are designed to form a stable interaction with conjugates and form a red line disregard to the presence or absence of the target. Finally, excess conjugates and sample liquids are brought to the wicking pad by capillary forces.

Albeit, historically, most conjugates and capture molecules in LFAs are antibodies, recently, there is an emerging interest in nucleic acid-based LFAs (NALFAs). Nucleic acids have numerous advantages over antibodies. Shelf lives of the antibody-based LFAs are limited due to the irreversible denaturation of antibodies. However, in the presence of required metal ions and pH [15], nucleic acids fold to their functional format just upon rehydration. In addition, chemical synthesis of nucleic acids provides an opportunity for wide range of modifications which is promising for further development of NALFAs. Besides, NALFAs provide a platform to recognize presence of specific DNA or RNA sequences, which is a property that antibody-based LFAs cannot present. NALFAs have been reported to recognize a wide range of targets including allergens [16], human blood serine protease, thrombin [7], human salivary biomarkers [3], microRNAs [17], toxins such as aflatoxin B1 [18] and ochratoxin A [19], pathogens such as *Escherichia coli* [20], viral [21] and microbial DNAs [22], drugs of abuse such as cocaine [23] and metal ions such as lead [24] and copper [25, 26].

In most NALFAs, immobilized capture DNA molecules at the surface of nitrocellulose membranes are biotinylated [27]. Biotinylated capture DNAs are pre-complexed with streptavidin prior to be printed on the test line and control lines [26]. Such system provides limits of detection at nano- and picomolar ranges [27]; however, dependence on application of modified DNAs increases the costs of development procedures. Considering emerging interests in development and application of LFAs, there is a demand to reduce the costs of LFA development, to assure possibility of test development on various targets [28]. Here, we report on a NALFA model system utilizing a biotin- and streptavidin-free capture lines. We defined a unique capture line as a model system of control and test lines in a standard NALFA. No specific target is analyzed here to maintain generality of the research. Figure 1 demonstrates the experimental setup for this study, showing the capture line as a model system.

In addition, proper formation of hydrogen bonds and maximized hybridization of oligonucleotide strands at the surface of nitrocellulose membrane are two important factors for the best performance of NALFAs. Liquid samples that are generally used as the rehydrating buffer (running buffer that contains the analyte) are various in regard to their ionic strength, pH, composition and presence of extra additives such as protein blockers, detergents and chaotropic and kosmotropic agents. Such variation may affect the intensity of the visual bands. Here, we also present an optimized rehydrating buffer for formation of the signal at our developed biotin- and streptavidin-free, hence "protein-free" capture line. The buffer that maximizes the band intensity for the model capture line is expected to maximize the intensities of control and test lines in a real NALFA.

Materials and methods

Chemicals

Gold (III) chloride trihydrate, tris (2-carboxyethyl) phosphine hydrochloride (TCEP), all buffers, detergents, bovine

serum albumin (BSA), polyethylene glycol (PEG) and thiolated DNA were purchased from Sigma-Aldrich, Shanghai, China. Capture DNA was purchased from SinaClone (Tehran, Iran). Nitrocellulose membranes (Hi-Flow Plus 120), sample pad (cellulose fiber), conjugate release pad (glass fiber), wicking pad (cellulose fiber) and 0.22-μm filters were purchased from Merck Millipore. The buffer mixes including PBS (20X: 0.24 M trisodium phosphate buffer pH 7.4, 2.74 M NaCl, 0.54 M KCl), SSC (20X: 0.30 M trisodium citrate buffer pH 7.0, 3.0 M NaCl) and borate buffer saline (BBS, 10X: 0.1 M borate buffer pH 8.2, 1.5 M NaCl) were prepared and diluted freshly. Appropriate amounts of extra additives were added to the buffer mixes, using 10X and 5X concentrated solutions.

Gold nanoparticle synthesis and characterization

Gold nanoparticles were synthesized using published procedures [29]. Shortly, all glasswares were washed with freshly made aqua regia (HNO_3/HCl, 3:1) for 30 min and then rinsed with copious amount of Milli-Q water (18.2 MΩ cm^{-1}). In a reflux system with 200-ml two-necked Becher, 98 ml Milli-Q water was boiled to start reflux. Then, 2 ml 50 mM $HAuCl_4$ and 10 ml 38.8 mM trisodium citrate were added sequentially to the stirred and refluxed system. The color of solution changed from yellow to deep red in 2 min. The system was refluxed for additional 20 min and finally brought to room temperature while still stirring. The synthesized gold nanoparticles were sonicated for 3 min in 55 °C and then filtered through a 0.22-μm filter and stored at room temperature in a dark glass container.

The molarity of the synthesized gold nanoparticles was calculated using Eq. 1, which is based on the method introduced by Liu et al. [30]. In the aforementioned equation, ρ is the density of face-centered cubic gold structures which is 19.3 g/cm^3, M is the atomic mass of gold which is 197 g/mol and r is the radius of gold nanoparticles in nanometer (half of the nanoparticle size, determined by dynamic light scattering). N_{total} is the amount of gold atoms in the solution and N_A is the Avogadro number, i.e., 6.022×10^{23}.

$$\text{Molarity} = \frac{N_{\text{Total}}}{\frac{4\pi}{3}.r^3.\frac{\rho}{M}VN_A} \quad (1)$$

DNA immobilization on gold nanoparticles

Thiolated DNA (C6-S-S-C6-AAAAAAAAAAGTAAAAC GACGGCCAGT) was reduced in the presence of 50 mM acetate buffer pH 5.2 and 1 mM TCEP for 1 h at room temperature [29]. Reduced thiolated DNA was conjugated to 10 nM gold nanoparticle for 16 h at room temperature in a glass tube which was first washed with aqua regia and then incubated with 12 N NaOH for 1 h at room temperature and then washed thoroughly with Milli-Q water and dried in 80 °C oven for 20 min. After overnight incubation, 10 μL Tris–acetate buffer pH 8.2 was added to the solution to reach final 5 mM concentration. The AuNP conjugates were aged with NaCl for additional 1 day. The aged AuNP conjugates were centrifuged for 20 min with 14,500 rpm at room temperature. The pallets were washed twice and got re-suspended in the re-suspension buffer (20 mM Na_3PO_4, 5% BSA, 0.25% Tween-20 and 10% sucrose).

LFA assembly and assay procedure

Prior to LFA assembly, capture DNA **I** (ACTGGCC GTCGTTTTAC) or capture DNA **II** (A40 ACTGGCCGT CGTTTTAC) was placed on the nitrocellulose membrane. One μL of single-stranded capture DNA with a concentration of 50 μM (except otherwise mentioned) was printed on nitrocellulose membrane as reported by Jauset-Rubio et al. [31]. The loaded DNA was dried in 70 °C for 30 min. In the case of control experiments with biotinylated DNA, 20 μL of 1 mM biotinylated capture DNA (biotin-ACTGGCCGTCGTTTTAC) and 2 mg/ml streptavidin (200 μL) were incubated at room temperature for 1 h. Then, 500 μL PBS was added and sample was centrifuged for 6000 rpm for 20 min at 4 °C. The pallet was washed one more time with 500 μL PBS and finally was dissolved in 100 μL of PBS. Thus, the final concentration of the biotinylated DNA–streptavidin complex was maximally 200 μM.

In parallel, gold nanoparticle–DNA conjugates were dispensed on conjugate release pad and were dried by air flow at room temperature. For LFA assembly, firstly, dried nitrocellulose membranes were attached on an adhesive polyester backing card. Conjugate release pad and sample pad were attached on the next layers with 2-mm overlap with the nitrocellulose membrane, to accommodate lateral flow. On the other end of the nitrocellulose membrane, the wicking pad was attached with 2-mm overlap.

The assembled test strips were placed into a plastic holder, and 50 μL of rehydrating buffer was loaded on sample pad. After 2–5 min, the bands were clearly visible. The strips were dried by air flow and scanned with Epson perfection V37 scanner. All the tests were repeated three times at room temperature, 25 °C. The intensity of the bands was analyzed with ImageJ program. The intensity of the signal in the presence 1X PBS was taken as standard (100%), and any other results were normalized accordingly (except in Fig. 2A). Significant differences between measurements were analyzed with two-tailed t-tests using Origin pro 8 program with p value < 0.05. In Table 1, the impact of the additives (IOA) on the signal intensities was calculated as Eq. 2. Improvement in signal was defined with positive IOA, and decrement in the signal intensity was defined with negative IOA.

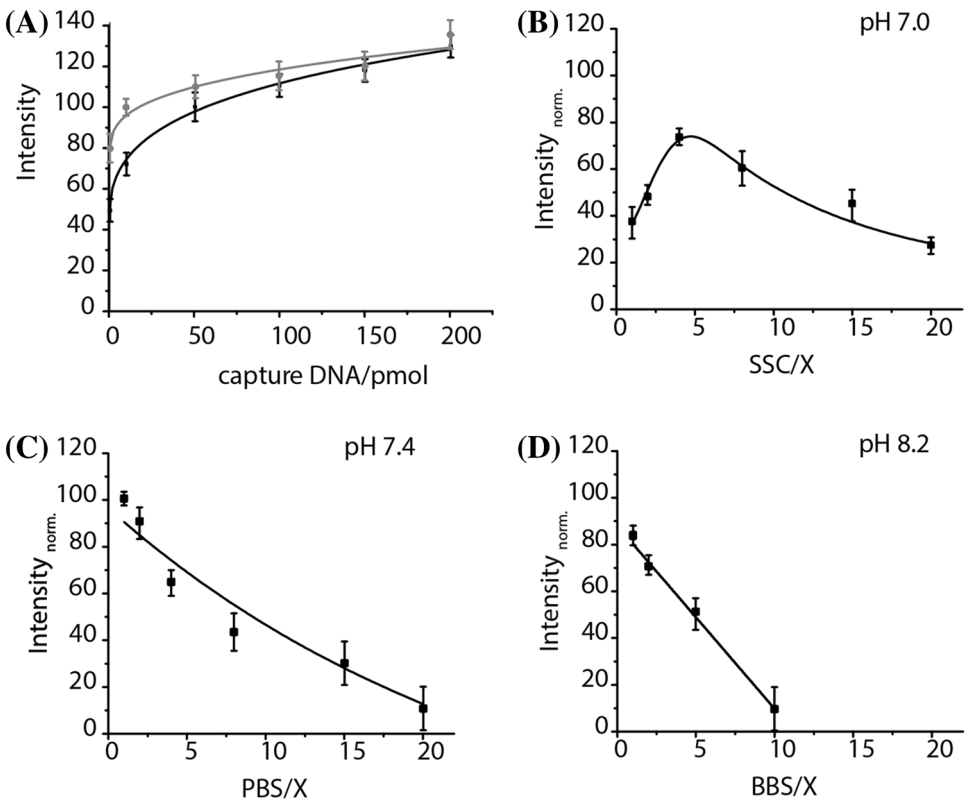

Fig. 2 Capture DNA titration and the effect of running buffers. (**A**) Intensity of the capture line with increasing concentration of the capture DNA. The tests were run with 1X PBS as running buffer. Tailed capture DNA (black) or complex of biotinylated capture DNA with streptavidin (gray) was loaded in the volume of 1 µL. (**B**), (**C**) and (**D**) Titration of saline sodium citrate buffer, phosphate buffer saline and borate buffer saline as running buffers. Capture line contained 1 µL of 50 nM tailed capture DNA. 1X PBS showed highest intensity and was chosen as standard (100%). Every other intensities are reported as the percentage of 1X PBS. Indicated error bars are standard deviation

$$\text{IOA} = \text{signal in the presence of additive} / \text{signal in the absence of additive} \quad (2)$$

Curve fitting

Logistic curve was fit to the capture line titration data. Exponential decay curves were fit to the PBS and BBS titration data and blocker titration (in the presence of Tris pH 7.4). Gauss curves were fit to the SSC, NaCl and blocker titration data (in the presence of PBS and SSC). The fit formulas for logistic curves, exponential decay curves and Gauss curves are as Eqs. 3–5, respectively, where A–E are parametric fit values. All fits accommodated R-square above 0.90.

$$y = A + (B - A)/(1 + (x/C) \wedge D) \quad (3)$$

$$y = A * \exp(-x/B) + C \quad (4)$$

$$y = A + (B/(C * \text{sqrt}(D/2))) * \exp(-2 * ((x - E)/C) \wedge 2) \quad (5)$$

Results

Development of the capture line with non-biotinylated DNA

In the first step, non-modified 17 nucleotides long capture DNA I was printed on the surface of nitrocellulose membrane (10–500 pmol, 1 µL of the appropriate concentration). No signal was achieved in the presence of any buffer setups. Absence of signal raised two hypotheses: either (1) the capture DNA I and its complement, i.e., the conjugated DNA, do not form proper hybridization or (2) the hybrid dsDNA is formed but the complexed is washed away from nitrocellulose membrane. To address these questions, capture DNA II was designed and investigated. Capture DNA II had the same sequence as DNA I except an A40 tail at its 5′ end. In contrast to DNA I, signals at the capture line have got visible using DNA II in the absence of any biotin–streptavidin interaction. With the successful achievement on visualization of the biotin- and streptavidin-free capture line, we aimed to optimize the density of the biotinylated capture DNA, DNA II. Increasing concentrations of capture DNA II was printed on nitrocellulose membrane. The assays were run with 1X PBS. The intensity of the capture line was increased logistically upon increase in capture DNA II concentration (Fig. 2A). According to the outcome of the capture DNA titration, 50 pmol capture DNA II was chosen for the next optimization experiments. As a control, biotinylated capture DNA (17 nucleotides long and untailed) was analyzed besides. The intensities of the control experiment signals were comparable with the signal intensities of tailed DNA, DNA II.

Table 1 The impact of additives (IOA) in the rehydrating buffers

	pH	SDS (%)	SDS+BSA (%)	Triton X-100 (%)	Tween-20 (%)	Urea (%)	PEG-6000 (%)	PEG-4000 (%)
SSC	7.0	+74	+92	−79	−81	−77	−81	−76
PBS	7.4	+73	+97	−91	−98	−48	−76	−99
Tris	7.4	+21	+22	−58	−59	−44	−47	−58
BBS	8.2	+62	+95	−90	−92	−58	−86	−92

Signal intensities have been analyzed by ImageJ as described in "Materials and methods"

BBS: 1X; PBS: 1X; SSC: 4X; Tris: 10 mM pH 7.4; SDS: 1%; BSA: 4%; urea: 1%; PEG-4000 and 6000: 1%; Tween-20: 1%

Influence of pH and composition of the rehydrating buffer

Three different buffer systems were chosen as running buffers: sodium saline citrate buffer (SSC, pH 7.0), phosphate buffer saline (PBS, pH 7.4) and borate buffer saline (BBS, pH 8.2). SSC, PBS and BBS were chosen since they are widely used in LFA tests. In addition, pH above 8.0 was reported to improve DNA–DNA hybridization efficiencies at special surfaces [32]. Hence, we aimed to investigate the effect of pH 8.2 (BBS) on the hybridization efficiency at the surface of nitrocellulose membrane. The 1X mixes of the three buffer systems contained similar buffer concentration, i.e., 10 mM buffer for SSC and BBS and 12 mM buffer for PBS. In addition, the ionic strengths of all three were within the same range. The 1X SSC and BBS had 150 mM NaCl and 1X PBS contained 137 mM NaCl and 2.7 mM KCl. Hence, the main difference among the 1X buffer mixes was their pH.

Our result showed that upon increase in the concentration fold of PBS and BBS, the intensity of the capture line was reduced exponentially (Fig. 2C, D). The decrease was more dramatic in the case of BBS. With 10X BBS, almost no capture line was visible. In contrast to PBS and BBS, the titration curve for SSC followed a Gauss model and had a maximum peak at 4X SSC (Fig. 2B). Presence of a maximum peak about 4X SSC was in agreement with previous reports on biotin–streptavidin-based NALFAs [26, 33].

Our data showed that, however, 1X solutions of the applied buffers have similar ionic strength and also similar buffer concentrations; the intensities of the capture lines were significantly different. Significance analysis was characterized by p value using two-tailed t-tests (p value < 0.05).

Improvement in signal versus background

The signal-to-noise ratio of the model NALFA was improved by three means, i.e., addition of a protein blocker, optimization of ionic strength and utilizing detergents and chaotropic and kosmotropic agents. Most LFA reports apply BSA as a blocker agent. BSA forms non-specific contacts to the surface of the nitrocellulose and avoids formation of such contacts by conjugates. We titrated increasing concentrations of BSA in the presence of 1X PBS, 4X SSC and 10 mM Tris–HCl pH 7.4. Our result showed that in the presence of saline buffers (SSC and PBS), BSA reduces the background and improves the band intensities when it is applied up to an optimal concentration of 4% w/v (Fig. 3A, B). Further increase in concentration of BSA had an inverse effect and increased background. In addition, high concentrations of the blocker (6% and above) caused formation of subtle cracks in the nitrocellulose membrane that caused channeling and altered even flow of the buffer. In the case of un-saline buffer (10 mM Tris–HCl, pH 7.4), the crackles were more drastic and the signal intensities were dramatically lower than saline buffers (Fig. 3C).

In the next step, we addressed the effect of the ionic strength on the visibility of the capture line versus background. NaCl was titrated in the presence of phosphate buffer, and the band intensities were compared and normalized to 1X PBS (Fig. 4A). The result showed a Gaussian behavior with an optimal NaCl concentration of ca. 120 mM. Concentrations above the optimal caused an increase in the background and therefore reduced the capture line intensities versus background.

Detergents are known to reduce background in LFAs. They inhibit non-specific attachment of gold nanoparticle conjugates to the nitrocellulose membrane. We investigated the effect of the presence of ionic, nonionic and chaotropic detergents (1% each) in the running buffer. Sodium dodecyl sulfate (SDS) was used as a candidate for ionic detergents, Triton X-100 and Tween-20 were used as examples of nonionic detergents, and urea was added as a chaotropic detergent. Our result showed that ionic detergent SDS (1%) improved the signal intensity up to 75%. The best effect was observed for SSC and PBS buffer. SDS had the least improvement effect in the presence of 10 mM Tris pH 7.4. Simultaneous presence of BSA and SDS could increase the signal up to 97%. As an example, the signal

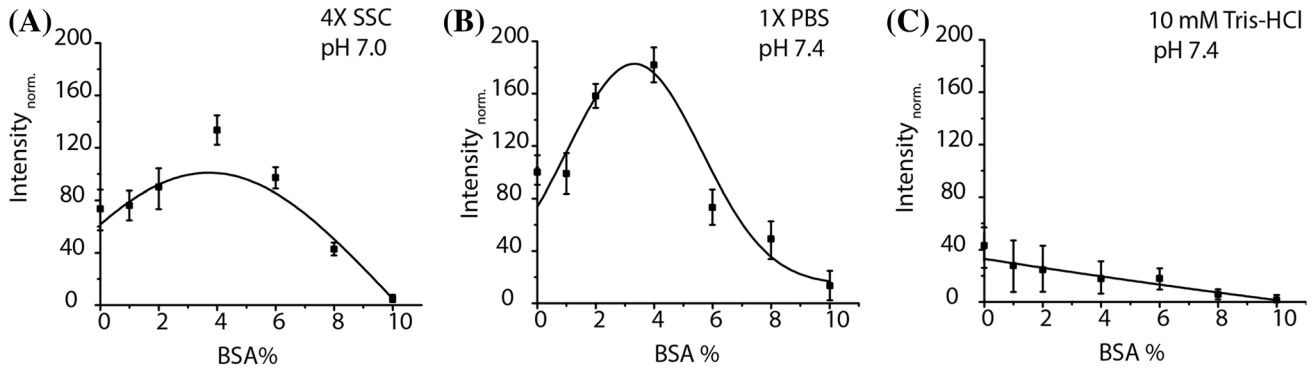

Fig. 3 Titration of blocking agent. Titration of BSA as a blocking agent in the presence of 4X SSC (**A**), 1X PBS (**B**) and 10 mM Tris–HCl pH 7.4 (**C**). The horizontal axes show percentage (w/v%) of the blocker in the running buffer. While for saline buffers (SSC and PBS), 4% w/v blocker increased visibility of the capture line, in the presence of similar concentration and pH of Tris buffer (and in the absence of NaCl), blocker reduced the signal dramatically. Intensities are represented as a percentage of the intensity of the capture line with PBS 1X running buffer. Indicated error bars are standard deviation

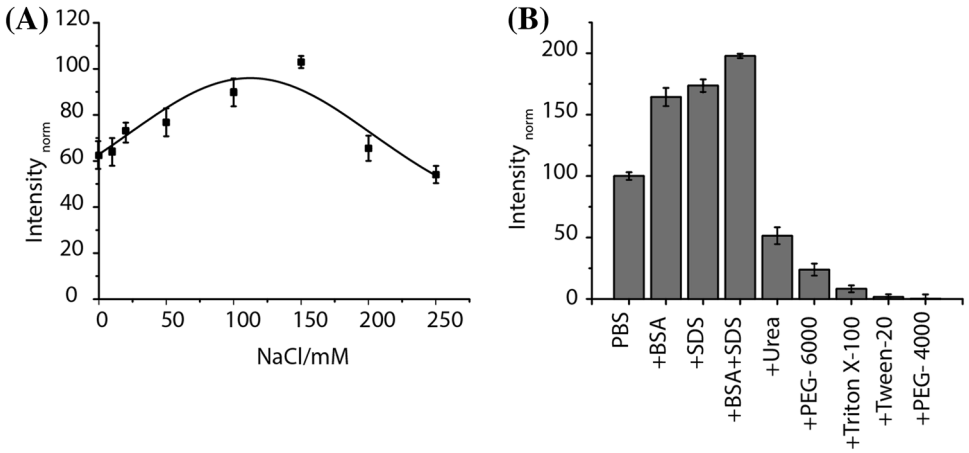

Fig. 4 The effect of ionic strength and additives. (**A**) Ionic strength effect on the visibility of the capture line. NaCl titrated to 12 mM phosphate buffer pH 7.4 and used as running buffer. The band intensities were normalized against 1X PBS. (**B**) The effect of detergents and chaotropic and kosmotropic agents on the visibility of the capture line. PBS: 1X; BSA: 4%; SDS: 1%; urea: 1%; PEG-4000 and 6000: 1%; Tween-20: 1%. Indicated error bars are standard deviation

intensity of the test with 1X PBS in the presence of 1% SDS and 4% BSA as running buffer was almost twice of the signal intensity of the band when 1X PBS was used solely. This effect was least visible for Tris 10 mM pH 7.4. Addition of nonionic detergents, Triton X-100 and Tween-20, reduced the signal intensity up to 90%. The effects were less harsh in the case of 10 mM Tris pH 7.4. Chaotropic detergent, urea, reduced the signal intensity by 77%. The worse effect was for 4X SSC buffer, and the least harsh effect was for 10 mM Tris pH 7.4 (Table 1).

Molecular crowders such as PEG cause an increase in the effective concentrations of the macromolecules by excluded volume effect and have been shown to facilitate hybridization of oligonucleotides [34]. Hence, we applied PEG-4000 and PEG-6000 as an additive to the buffer systems. Addition of 1% PEG-4000 or PEG-6000 reduced the signal at the capture line. The reduction in signal was due to the increased background. Figure 4B and Table 1 summarize the results of addition of detergents and molecular crowders to the 1X PBS.

Discussion

In conclusion, nucleic acid-based lateral flow assays (NALFA) have great potential on detection of DNA sequences and target analyte. Regarding public health, hybridization-based NALFAs have been proven to detect DNA molecules form pathogens in food and water [35]. Aptamer-based NALFAs have shown to detect toxins [18, 19], and deoxyribozyme-based NALFA has proven to sense metal ions [36]. Regarding clinical aspects, they have been shown to be useful in genotyping [37], single nucleotide polymorphism detection [38] and diagnosing

health biomarkers [17]. To the best of our knowledge, all reports on NALFA apply modified forms of nucleic acids on the surface of the nitrocellulose membrane. Here, we reported on development of a model protein-free NALFA with non-modified capture DNA and introduced an optimum rehydrating buffer for such system.

Visibility of a capture line in hybridization-based NALFAs depends on two main factors: (1) efficient DNA hybridization and (2) immobility of the formed dsDNA on the nitrocellulose membrane. Regarding the former, efficiency of duplex formation is a function of several factors such as temperature, buffer composition, concentration and pH, ionic strength, presence of organic molecules and length, sequence and concentration of capture and conjugate DNAs. Regarding the latter, in a NALFA experiment, the possibility of lateral migration of the formed dsDNA with sample liquid must be noted. Such possible migration prevents visualization of the capture line, although the duplex DNA may be formed.

Here, applying a short capture DNA (DNA I, 17 mer) resulted in no signal, while addition of a tail with the length of 40 nucleotides at the 5′ end of the same sequence (DNA II, 57 mer) leads to visible line that was detectable with naked eyes. The two DNAs were designed to form equal length of duplex with conjugate DNA ($T_m = 62$ °C). In the other words, the 40-nucleotide tail at 5′ end of DNA II did not contribute on formation of any duplex DNA. Therefore, improvement in the signal visibility with DNA II was attributed to the fact that higher molecular weight of the complex, i.e., higher size of the DNA complex, restrained lateral migration of the complex from capture line. The lowest amount of DNA II that formed a visible band at the capture line was 10 pmol (1 μL of 10 μM DNA II). One should notice that this is the concentration limit for the immobilized capture line and does not reflect the limit of the detection of the system. Here, a model capture line was presented with no specific target. Hence, the definition of a detection limit is due when this system is applied for detection of specific analyte.

Consequently, in this report, we analyzed the effect of various buffers ranging from citrate to phosphate and boric acid, pH 7.0 to 8.2, on the intensity of the capture line in the presence of various ionic strengths, 0–250 mM monovalent ions and extra additives such as detergents, chaotropes and kosmotropes, 1–4%.

Our results showed that buffers with similar concentration (ca. 10 mM) and ionic strength (150 mM monovalent ions) but different pH have significant distinct effect on the visibility of the capture line. PBS pH 7.4 showed highest signals in comparison with BBS pH 8.2 and SSC pH 7.0. We observed that an increase in the fold concentrations of buffer mixes of PBS and BBS reduces the signal intensity, since the background is increased. This is explained with the fact that high fold concentrations facilitate non-specific contacts of conjugates to the nitrocellulose membrane and thus there is less conjugate available for formation of the double-stranded DNA duplex at the capture line. In addition, high background reduces the contrast at the capture line. In the case of SSC buffer, the optimal concentration fold was 4. The same effect was reported previously on biotin–streptavidin-dependent NALFAs [26, 33] and could be explained by lower pH of SSC in comparison with PBS and BBS since the adsorption efficiency of the capture DNA to the surface of nitrocellulose is pH dependent [28].

Monovalent metal ions have been shown to affect the visibility of the capture line. Their role in screening the negative charges of the phosphate backbone of DNA strands is understandable [39]. However, we showed that the optimal ionic strength depends on the pH of the rehydrating buffer. NaCl concentration ca. 150 mM resulted in highest signal for buffers with pH 7.4 and 8.2; however, for SSC buffer with pH 7.0, 4X SCC with 600 mM NaCl had best performance. Thus, the ionic strength showed a positive effect up to an optimal concentration and the optimal concentration is under the control of buffer pH.

To reduce non-specific interaction of DNA–AuNP conjugate to the nitrocellulose membrane, a protein blocker is often used [7]. Here, we demonstrated that 4% BSA has most improvement in the presence of saline buffers. BSA has a size of 7.5 nm × 6.5 nm × 4 nm [40]. Appropriate concentrations of BSA can embed on the surface of nitrocellulose without clogging the pores. However, higher BSA concentration may block the nitrocellulose pores and interfere with even flow of conjugate and thus increases the background.

To minimize background in our developed NALFA model, we included detergents and chaotropic and kosmotropic agents in the rehydrating buffer. The ionic detergent SDS improved the signal intensity. The effect was in positive cooperation with BSA as well. The non-ionic detergent Triton X-100 reduced the signal intensity. This observation was in contrast to a report by Mashayekhi et al. [41]. The system introduced by Mashayekhi used concentrations of Triton X-114 above critical micelle concentration; however, the concentrations in this report and in many LFA reports are much below the critical micelle concentrations of any detergent.

The effect of the chaotropic detergent, urea, was as expected. Urea is known to disrupt hydrogen bonding [42], and therefore, it was expected to decrease the hybridization of the capture DNA and the conjugate. In contrast to urea, the kosmotropic agent, PEG [43], could have contradictory effects. It could help DNA–DNA interaction and formation of the DNA duplex at the capture line. In aqueous solutions, PEG molecules are strongly hydrated and thus the amount of water molecule available for hydration of any

other molecule in solution is decreased. Hence, PEG is considered as a crowder molecule. This phenomenon increases the effective concentrations of other molecules in the system, here capture DNA and conjugates. Presence of PEG and increase in the effective concentrations of oligonucleotides are expected to improve dsDNA formation. In the other hand, PEG could increase the formation of non-specific contacts between the conjugates and nitrocellulose membrane. Increased background of the tests, in the presence of PEG-4000 and 6000, and loss of contrast at the capture line pointed that the second effect was more pronounced at the applied conditions.

In summary, we showed that with a long enough capture DNA, there is no need of biotinylation and formation of streptavidin–biotinylated DNA complex for capture DNA. Utilizing unmodified capture DNAs reduces development costs for NALFAs and provides opportunities for fast and cost-effective development of NALFAs for any target. Herein, we presented a protein-free NALFA model system using an unmodified capture DNA. We also optimized rehydration buffer for such system, and we concluded that 1X PBS (12 mM phosphate buffer pH 7.4, 137 mM NaCl, 2.7 mM KCl) in the presence of 1% SDS and 4% BSA is the best rehydrating buffer for biotin- and streptavidin-free hybridization-based NALFAs. These conditions can be utilized for further development of point of care tests that are based on nucleic acid on the surface of nitrocellulose membranes including genosensing dipsticks and isothermal amplification-based lateral flow assays [44].

Acknowledgments Financial support from university of Isfahan is acknowledged. The author thanks Prof. Dr. Claudia Höbartner to supply thiolated DNA for this project.

References

1. Gubala V, Harris LF, Ricco AJ, Tan MX, Williams DE (2011) Point of care diagnostics: status and future. Anal Chem 84(2):487–515
2. Lee S, O'Dell D, Hohenstein J, Colt S, Mehta S, Erickson D (2016) NutriPhone: a mobile platform for low-cost point-of-care quantification of vitamin B12 concentrations. Sci Rep 6:28237. doi:10.1038/srep28237
3. Minagawa H, Onodera K, Fujita H, Sakamoto T, Akitomi J, Kaneko N, Shiratori I, Kuwahara M, Horii K, Waga I (2017) Selection, characterization and application of artificial DNA aptamer containing appended bases with sub-nanomolar affinity for a salivary biomarker. Sci Rep 7:42716. doi:10.1038/srep42716
4. Li Z, Wang Y, Wang J, Tang Z, Pounds JG, Lin Y (2010) Rapid and sensitive detection of protein biomarker using a portable fluorescence biosensor based on quantum dots and a lateral flow test strip. Anal Chem 82(16):7008–7014
5. Khreich N, Lamourette P, Boutal H, Devilliers K, Créminon C, Volland H (2008) Detection of Staphylococcus enterotoxin B using fluorescent immunoliposomes as label for immunochromatographic testing. Anal Biochem 377(2):182–188
6. Anfossi L, Di Nardo F, Giovannoli C, Passini C, Baggiani C (2013) Increased sensitivity of lateral flow immunoassay for ochratoxin A through silver enhancement. Anal Bioanal Chem 405(30):9859–9867
7. Xu H, Mao X, Zeng Q, Wang S, Kawde A-N, Liu G (2009) Aptamer-functionalized gold nanoparticles as probes in a dry-reagent strip biosensor for protein analysis. Anal Chem 81(2):669–675. doi:10.1021/ac8020592
8. Yang Q, Gong X, Song T, Yang J, Zhu S, Li Y, Cui Y, Zhang B, Chang J (2011) Quantum dot-based immunochromatography test strip for rapid, quantitative and sensitive detection of alpha fetoprotein. Biosens Bioelectron 30(1):145–150. doi:10.1016/j.bios.2011.09.002
9. Gandhi S, Caplash N, Sharma P, Raman Suri C (2009) Strip-based immunochromatographic assay using specific egg yolk antibodies for rapid detection of morphine in urine samples. Biosens Bioelectron 25(2):502–505. doi:10.1016/j.bios.2009.07.018
10. Grothaus GD, Bandla M, Currier T, Giroux R, Jenkins GR, Lipp M, Shan G, Stave JW, Pantella V (2006) Immunoassay as an analytical tool in agricultural biotechnology. J AOAC Int 89(4):913–928
11. Choi JR, Hu J, Tang R, Gong Y, Feng S, Ren H, Wen T, Li X, Wan Abas WA, Pingguan-Murphy B, Xu F (2016) An integrated paper-based sample-to-answer biosensor for nucleic acid testing at the point of care. Lab Chip 16(3):611–621. doi:10.1039/c5lc01388g
12. Orlov AV, Znoyko SL, Cherkasov VR, Nikitin MP, Nikitin PI (2016) Multiplex biosensing based on highly sensitive magnetic nanolabel quantification: rapid detection of botulinum neurotoxins A, B, and E in liquids. Anal Chem 88(21):10419–10426. doi:10.1021/acs.analchem.6b02066
13. Corstjens PLAM, Zuiderwijk M, Nilsson M, Feindt H, Sam Niedbala R, Tanke HJ (2003) Lateral-flow and up-converting phosphor reporters to detect single-stranded nucleic acids in a sandwich-hybridization assay. Anal Biochem 312(2):191–200. doi:10.1016/S0003-2697(02)00505-5
14. Yu HLL, Montesa CM, Rojas NRL, Enriquez EP (2012) Nucleic-acid based lateral flow strip biosensor via competitive binding for possible dengue detection. J Biosens Bioelectron 3(5):128–134. doi:10.4172/2155-6210.1000128
15. Chen A, Yang S (2015) Replacing antibodies with aptamers in lateral flow immunoassay. Biosens Bioelectron 71:230–242. doi:10.1016/j.bios.2015.04.041
16. Jauset-Rubio M, Svobodova M, Mairal T, McNeil C, Keegan N, El-Shahawi MS, Bashammakh AS, Alyoubi AO, O'Sullivan CK (2016) Aptamer lateral flow assays for ultrasensitive detection of beta-conglutin combining recombinase polymerase amplification and tailed primers. Anal Chem 88(21):10701–10709. doi:10.1021/acs.analchem.6b03256
17. Kor K, Turner AP, Zarei K, Atabati M, Beni V, Mak WC (2016) Structurally responsive oligonucleotide-based single-probe lateral-flow test for detection of miRNA-21 mimics. Anal Bioanal Chem 408(5):1475–1485
18. Shim WB, Kim MJ, Mun H, Kim MG (2014) An aptamer-based dipstick assay for the rapid and simple detection of aflatoxin B1. Biosens Bioelectron 62:288–294. doi:10.1016/j.bios.2014.06.059
19. Wang L, Ma W, Chen W, Liu L, Zhu Y, Xu L, Kuang H, Xu C (2011) An aptamer-based chromatographic strip assay for sensitive toxin semi-quantitative detection. Biosens Bioelectron 26(6):3059–3062. doi:10.1016/j.bios.2010.11.040
20. Bruno JG (2014) Application of DNA aptamers and quantum dots to lateral flow test strips for detection of foodborne pathogens with improved sensitivity versus colloidal gold. Pathogens (Basel, Switzerland) 3(2):341–355. doi:10.3390/pathogens3020341

21. Xu Y, Liu Y, Wu Y, Xia X, Liao Y, Li Q (2014) Fluorescent probe-based lateral flow assay for multiplex nucleic acid detection. Anal Chem 86(12):5611–5614
22. Huang HL, Zhu P, Zhou CX, He S, Yan XJ (2017) The development of loop-mediated isothermal amplification combined with lateral flow dipstick for detection of Karlodinium veneficum. Harmful Algae 62:20–29. doi:10.1016/j.hal.2016.11.022
23. Liu J, Mazumdar D, Lu Y (2006) A simple and sensitive "dipstick" test in serum based on lateral flow separation of aptamer-linked nanostructures. Angew Chem 118(47):8123–8127
24. Mazumdar D, Liu J, Lu G, Zhou J, Lu Y (2010) Easy-to-use dipstick tests for detection of lead in paints using non-cross-linked gold nanoparticle-DNAzyme conjugates. Chem commun (Cambridge, England) 46(9):1416–1418. doi:10.1039/b917772h
25. Fang Z, Huang J, Lie P, Xiao Z, Ouyang C, Wu Q, Wu Y, Liu G, Zeng L (2010) Lateral flow nucleic acid biosensor for Cu^{2+} detection in aqueous solution with high sensitivity and selectivity. Chem commun (Cambridge, England) 46(47):9043–9045. doi:10.1039/c0cc02782k
26. Wang Y, Wang L, Xue J, Dong J, Cai J, Hua X, Wang M, Zhang C, Liu F (2017) Signal-amplified lateral flow test strip for visual detection of Cu^2. PLoS ONE 12(1):e0169345. doi:10.1371/journal.pone.0169345
27. Wang X, Choi N, Cheng Z, Ko J, Chen L, Choo J (2017) Simultaneous detection of dual nucleic acids using a SERS-based lateral flow assay biosensor. Anal Chem 89(2):1163–1169. doi:10.1021/acs.analchem.6b03536
28. Holstein CA, Chevalier A, Bennett S, Anderson CE, Keniston K, Olsen C, Li B, Bales B, Moore DR, Fu E, Baker D, Yager P (2016) Immobilizing affinity proteins to nitrocellulose: a toolbox for paper-based assay developers. Anal Bioanal Chem 408(5):1335–1346. doi:10.1007/s00216-015-9052-0
29. Liu J, Lu Y (2006) Preparation of aptamer-linked gold nanoparticle purple aggregates for colorimetric sensing of analytes. Nat Protoc 1(1):246
30. Liu X, Atwater M, Wang J, Huo Q (2007) Extinction coefficient of gold nanoparticles with different sizes and different capping ligands. Colloids Surf B Biointerfaces 58(1):3–7. doi:10.1016/j.colsurfb.2006.08.005
31. Jauset-Rubio M, Svobodova M, Mairal T, McNeil C, Keegan N, Saeed A, Abbas MN, El-Shahawi MS, Bashammakh AS, Alyoubi AO, O' Sullivan CK (2016) Ultrasensitive, rapid and inexpensive detection of DNA using paper based lateral flow assay. Sci Rep 6:37732. doi:10.1038/srep37732
32. Zhang J, Lang HP, Yoshikawa G, Gerber C (2012) Optimization of DNA hybridization efficiency by pH-driven nanomechanical bending. Langmuir 28(15):6494–6501. doi:10.1021/la205066h
33. Carter DJ, Cary RB (2007) Lateral flow microarrays: a novel platform for rapid nucleic acid detection based on miniaturized lateral flow chromatography. Nucleic Acids Res 35(10):e74
34. Kilburn D, Roh JH, Guo L, Briber RM, Woodson SA (2010) Molecular crowding stabilizes folded RNA structure by the excluded volume effect. J Am Chem Soc 132(25):8690–8696. doi:10.1021/ja101500g
35. Tang R, Yang H, Gong Y, You M, Liu Z, Choi JR, Wen T, Qu Z, Mei Q, Xu F (2017) A fully disposable and integrated paper-based device for nucleic acid extraction, amplification and detection. Lab Chip. doi:10.1039/c6lc01586g
36. Mazumdar D, Lan T, Lu Y (2017) "Dipstick" colorimetric detection of metal ions based on immobilization of DNAzyme and gold nanoparticles onto a lateral flow device. Methods Mol Biol (Clifton, NJ) 1571:389–406. doi:10.1007/978-1-4939-6848-0_24
37. Yu L, Wu W, Lie P, Liu Y, Zeng L (2013) Isothermal strand-displacement polymerase reaction for visual detection of the southeast asian-type deletion of α-thalassemia. J Mol Diagn 15(6):776–782
38. Zeng L, Xiao Z (2017) A lateral flow biosensor for the detection of single nucleotide polymorphisms. Methods Mol Biol (Clifton, NJ) 1572:421–430. doi:10.1007/978-1-4939-6911-1_27
39. Sigel A, Sigel H, Sigel RK (2011) Structural and catalytic roles of metal ions in RNA. Metal Ions Life Sci 9(11):299–345
40. Erickson HP (2009) Size and shape of protein molecules at the nanometer level determined by sedimentation, gel filtration, and electron microscopy. Biol Proced Online 11:32–51. doi:10.1007/s12575-009-9008-x
41. Mashayekhi F, Chiu RY, Le AM, Chao FC, Wu BM, Kamei DT (2010) Enhancing the lateral-flow immunoassay for viral detection using an aqueous two-phase micellar system. Anal Bioanal Chem 398(7–8):2955–2961. doi:10.1007/s00216-010-4213-7
42. Ramakrishnan S, Krainer G, Grundmeier G, Schlierf M, Keller A (2016) Structural stability of DNA origami nanostructures in the presence of chaotropic agents. Nanoscale 8(19):10398–10405. doi:10.1039/c6nr00835f
43. Chen WY, Hsu MY, Tsai CW, Chang Y, Ruaan RC, Kao WH, Huang EW, Chuan HY (2013) Kosmotrope-like hydration behavior of polyethylene glycol from microcalorimetry and binding isotherm measurements. Langmuir 29(13):4259–4265. doi:10.1021/la304500w
44. Park BH, Oh SJ, Jung JH, Choi G, Seo JH, Kim DH, Lee EY, Seo TS (2017) An integrated rotary microfluidic system with DNA extraction, loop-mediated isothermal amplification, and lateral flow strip based detection for point-of-care pathogen diagnostics. Biosens Bioelectron 91:334–340